

Gyromagnetic bifurcation in a levitated ferromagnetic particle

T. Sato¹, T. Kato¹, Daigo Oue^{2,3,4} and M. Matsuo^{2,5,6,7}

¹*Institute for Solid State Physics, University of Tokyo, Kashiwa 277-8581, Japan*

²*Kavli Institute for Theoretical Sciences, University of Chinese Academy of Sciences, Beijing 100190, China*


³*The Blackett Laboratory, Imperial College London, London SW7 2AZ, United Kingdom*

⁴*Instituto de Telecomunicações, Instituto Superior Técnico, University of Lisbon, 1049-001 Lisboa, Portugal*

⁵*CAS Center for Excellence in Topological Quantum Computation, University of Chinese Academy of Sciences, Beijing 100190, China*

⁶*Advanced Science Research Center, Japan Atomic Energy Agency, Tokai 319-1195, Japan*

⁷*RIKEN Center for Emergent Matter Science (CEMS), Wako, Saitama 351-0198, Japan*

 (Received 4 February 2022; revised 11 May 2023; accepted 15 May 2023; published 30 May 2023)

We examine the mechanical rotation of a levitated magnetic particle that is induced by ferromagnetic resonance under microwave irradiation. We show that two stable solutions appear in a certain range of parameters by bifurcation when the rotation frequency is comparable to the microwave frequency. This phenomenon originates from the coexistence of the Barnett and the Einstein–de Haas effects. We also reveal that this measurement is sensitive to the strength of the spin-rotation coupling. Our work provides a platform for accessing a microscopic relaxation process from spin to macroscopic rotation.

DOI: [10.1103/PhysRevB.107.L180406](https://doi.org/10.1103/PhysRevB.107.L180406)

Introduction. The discovery of gyromagnetism [1,2], i.e., the interconversion between spin and mechanical rotation, was a milestone in magnetism research, because it revealed the origin of magnetism to be the intrinsic angular momentum of electrons, which classical physics cannot explain, even before the establishment of quantum mechanics. Originally, gyromagnetic effects were investigated in bulk magnetic materials with the aim of determining their gyromagnetic ratios [3]. Recently, gyromagnetic effects have been recognized as universal phenomena, as demonstrated in various systems at scales ranging from those of condensed matter [4–16] to those of particle physics [17–21]. They have also provided powerful tools with which to measure and control both the mechanical and magnetic degrees of freedom [4,5,22–27].

Indeed, the Barnett effect (conversion of angular momentum of mechanical rotation into spin [1]) has been utilized to identify the angular-momentum compensation temperature of ferrimagnets [24,25] and to generate spin current from rigid-body rotation [6–8], surface acoustic waves [13–15], and vorticity in fluids [9–12]. On the other hand, the Einstein–de Haas effect (mechanical torque generated from spin polarization [2]), which is abbreviated as the EdH effect hereafter, has been utilized to measure the faint torque caused by a single-electron spin flip [23], identify the gyromagnetic ratio of a nanomagnetic thin film [22], and reveal the demagnetization process in ferromagnets on subpicosecond timescales [26].

Very recently, it has been demonstrated, in a solid-state device, that the Barnett and EdH effects can coexist in the GHz-frequency regime [16], although the Barnett and EdH effects have been treated independently so far. Through these two routes, angular momenta can bounce back and forth between magnetic and mechanical degrees of freedom in a single system; hence, their coexistence may bring out rich physics and possibly highlight the microscopic features of the spin-rotation coupling, the fundamental coupling between

spin and mechanical angular momentum of a rotating body [28,29]. However, solid-state platforms involve various excitations; hence, the gyromagnetic phenomena are damped by and could even be buried in, e.g., spin and charge transport and impurity scattering. In this sense, it is crucial to construct a platform that is detached from those relaxation paths and enables high-frequency, stable rotation.

Levitated optomechanics, inspired by laser tweezers, levitation, and cooling [30–34], can provide such a platform. The stable levitation of small particles has been demonstrated under a high vacuum through the use of, e.g., optical and radio-frequency forces [35]. In particular, with optical forces controlled by parametric feedback, the subkelvin cooling of the center-of-mass motion of small particles has been

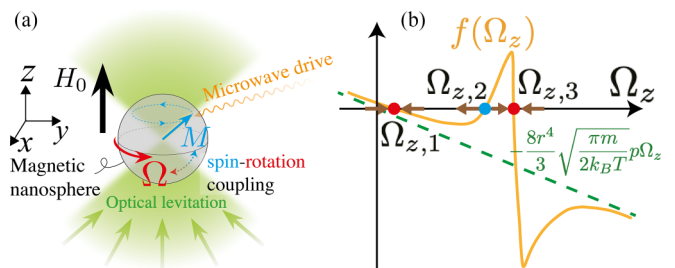


FIG. 1. (a) Schematic picture of the model. The magnetic nanosphere is optically levitated. The static magnetic field H_0 is applied in the z direction and the circularly polarized microwave field in the xy plane. They induce precession of the magnetization M and macroscopic rotation Ω about the z direction via the spin-rotation coupling. (b) Net angular-momentum gain $f(\Omega_z)$. There are three steady-state solutions, $\Omega_{z,i}$ ($i = 1, 2, 3$). For $\Omega_{z,1}$ and $\Omega_{z,3}$ (red points), an infinitesimal change in Ω_z produces a restoring torque, and thus the solutions become stable. In contrast, an infinitesimal deviation subsequently grows for $\Omega_{z,2}$, and thus that solution is unstable.

demonstrated [36–38]. By combining the feedback cooling scheme with the cavity cooling technique [39,40], even zero-point fluctuation of the center of mass has been revealed [41]. Since the motion of the center of mass can be significantly suppressed, the high-frequency rotation (\sim GHz) of small particles in a high vacuum has been studied recently [42–44,63]. The levitation of ferromagnets, which is necessary for our setup, has been studied theoretically in previous works [45–53] and has been achieved also experimentally [54,55]. Though the levitated optomechanical measurements are thus best suited for investigating the interplay between the Barnett and EdH effects, such an application has been overlooked so far.

In this Letter, we propose a levitated optomechanical setup to directly probe angular-momentum transfer between a spin system and mechanical rotation via Gilbert damping with high precision. We consider a small levitated particle and study its uniaxial rotation under microwave irradiation in a ferromagnetic resonance (FMR) experiment [see Fig. 1(a)]. We calculate the steady-state rotation frequency by balancing energy injection from microwaves and energy loss from air resistance and conclude that the particle can be rotated with a high rotation frequency up to GHz order in a vacuum. We show that the steady-state solution exhibits bifurcation when the rotation frequency is comparable to the microwave frequency, which is the requirement for the strong Barnett effect, in other words, coexistence of the Barnett and the EdH effects. The present setup enables us to sensitively measure the g factor in the spin-rotation coupling. Our result illustrates the usefulness of levitated optomechanical techniques in the study of gyromagnetism.

Dynamics of gyromagnetic systems. We consider a spherical ferromagnetic levitated particle of radius r , in which the motion of the center of mass is suppressed. For simplicity, the particle is regarded as a rigid body with a moment of inertia, $I = 2m_{\text{ptc}}r^2/5$, where m_{ptc} is the particle mass. We assume that the magnetization of the particle, \mathbf{M} , is initially directed in the z direction by an external static magnetic field. We consider a ferromagnetic resonance (FMR) experiment in which external microwaves irradiate a sample particle [56]. In this experiment, the angular momentum of the excited spins is transferred via the Gilbert damping to the rigid-body rotation of the particle and therefore the particle starts to rotate around the z axis. Its rotation frequency vector is denoted as $\boldsymbol{\Omega} = (0, 0, \Omega_z)$.

For the steady state, the Hamiltonian in the rotating frame fixed to the particle is written as [28,29,57]

$$\mathcal{H} = -(\mu_0\gamma\mathbf{H} + g_{\text{SR}}\boldsymbol{\Omega}) \cdot \hbar\mathbf{S}^{\text{tot}}. \quad (1)$$

The first term describes the Zeeman energy, where \mathbf{S}^{tot} is the total spin of the particle, μ_0 is the vacuum permeability, γ (<0) is the gyromagnetic ratio, and \mathbf{H} is the magnetic field in the rotating frame,

$$\mathbf{H} = \begin{pmatrix} h \cos(\omega - \Omega_z)t \\ h \sin(\omega - \Omega_z)t \\ H_0 \end{pmatrix}. \quad (2)$$

Here, H_0 is a static magnetic field and h ($\ll H_0$) and ω are the amplitude and frequency of the microwaves, respectively. The second term of the Hamiltonian (1) describes the spin-rotation

coupling that explains the Einstein–de Haas effect [2] and the Barnett effect [1]. Note that the g factor for the spin-rotation coupling, g_{SR} , generally deviates from one [55,57].

The magnetization of the particle is given as $\mathbf{M} = \hbar\gamma\mathbf{S}^{\text{tot}}/V$, where $V = 4\pi r^3/3$ is the volume of the particle. The Landau-Lifshitz-Gilbert (LLG) equation is given as

$$\dot{\mathbf{M}} = \mathbf{M} \times (\mu_0\gamma\mathbf{H} + g_{\text{SR}}\boldsymbol{\Omega}) + \frac{\alpha}{M_0}\mathbf{M} \times \dot{\mathbf{M}}, \quad (3)$$

where $M_0 = |\mathbf{M}|$, $\dot{\mathbf{M}} = d\mathbf{M}/dt$, and α is the Gilbert damping constant. The steady-state solution of the LLG equation can be obtained by assuming $\dot{M}_z = 0$ and $(M_x, M_y) = M(\cos[(\omega - \Omega_z)t + \phi], \sin[(\omega - \Omega_z)t + \phi])$ and using $M_0^2 = M^2 + M_z^2$. For this steady state, the z component of the gain rate of the angular momentum from the spin system is given as

$$[\mathbf{M} \times \mu_0\gamma\mathbf{H}]_z = -\frac{\alpha}{M_0}(\omega - \Omega_z)M^2. \quad (4)$$

This coincides with the Gilbert damping term $\alpha[\mathbf{M} \times \dot{\mathbf{M}}]_z/M_0$, indicating that the gain in angular momentum from the microwaves is lost through Gilbert damping. This spin relaxation causes continuous transfer of the angular momentum to the rigid-body angular momentum.

Magnetically driven rigid-body rotation. The equation for the time evolution of the angular momentum in the present system is given as [55]

$$\frac{d}{dt}[I\Omega_z + g_{\text{SR}}\hbar S_z^{\text{tot}}] = \Gamma_{\text{in}} + \Gamma_{\text{air}}, \quad (5)$$

where $\Gamma_{\text{in}} = \mu_0\gamma\hbar[\mathbf{S}^{\text{tot}} \times \mathbf{H}]_z$ is the torque supplied from the microwaves and Γ_{air} is the torque due to the air resistance (discussed later). When the Gilbert damping term is included phenomenologically as in the last term of Eq. (3), a steady state, $\dot{S}_z = 0$, arises from the balance between the Gilbert damping and the gain in angular momentum from the microwaves, Eq. (4). Then, Eq. (5) leads to the equation of motion for the steady-state rotation frequency Ω_z .

The steady-state rotation of the particle receives torque from the surrounding air. In this Letter, we focus on the molecular flow region in which $\lambda \gg r$ holds, where λ is the mean free path, in order to realize high-frequency rotation [43,58–60]. We assume diffuse reflection at the surface. Accordingly, the torque induced by the air resistance is calculated as [55]

$$\Gamma_{\text{air}} = -\frac{8r^4}{3}\sqrt{\frac{\pi m_{\text{air}}}{2k_{\text{B}}T}}\Omega_z p, \quad (6)$$

where m_{air} is the mass of the air molecules, k_{B} is the Boltzmann constant, T is temperature, and p is pressure. In the following estimate, we assume that the particle is in the atmosphere, for which the average molecular mass is $m_{\text{air}} = 4.78 \times 10^{-26}$ kg and take $r = 1 \times 10^{-6}$ m and $T = 273$ K [61]. The mean free path satisfies $p \cdot \lambda = k_{\text{B}}T/(\sqrt{2}\pi\xi^2)$, where ξ is the diameter of an air molecule. Substituting $\xi = 3.76 \times 10^{-10}$ m, we have $p \cdot \lambda \simeq 6.0 \times 10^{-3}$ N/m, and taking $p \lesssim 100$ Pa is sufficient to enter the molecular flow region $\lambda \gg r$.

Gyromagnetic bifurcation. First, we set $g_{\text{SR}} = 1$ in order to see the features of the steady-state rotation. The Euler equation of a spherical particle is presented in Eq. (5). Defining the net angular-momentum gain as $f(\Omega_z) \equiv$

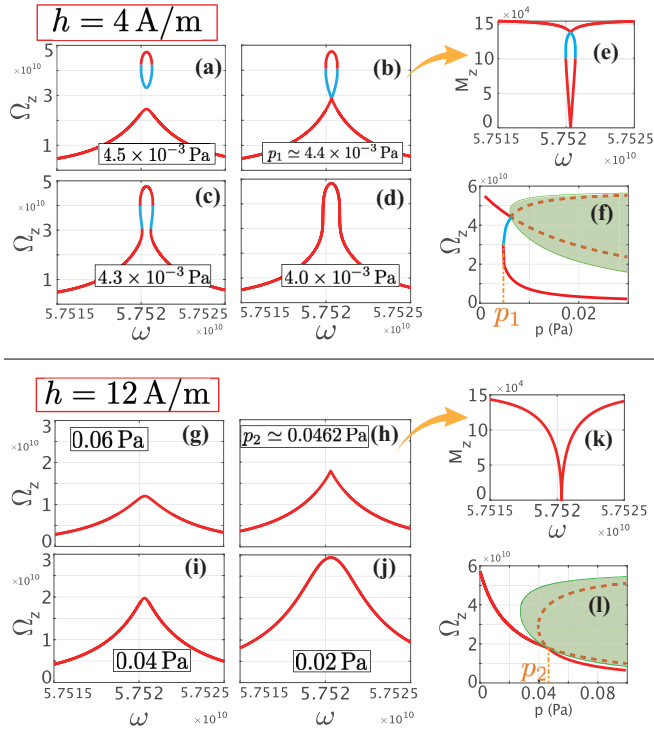


FIG. 2. Steady-state rotation frequency Ω_z for various pressures with microwave amplitudes (a)–(d) 4 A/m and (g)–(j) 12 A/m. (e), (k) The steady-state solutions of the magnetization M_z that correspond to Ω_z in (b) and (h), respectively. (f), (l) Red and blue curves express the p dependence of the steady-state solutions for the rotation frequency. The green area is the region in which the z component of the magnetization M_z becomes imaginary. Thus, the physical solutions are the red curves, and the solutions depicted by the blue curves are unstable.

$\Gamma_{\text{in}}(\Omega_z) + \Gamma_{\text{air}}(\Omega_z)$, the rotation frequency of the steady state can be obtained by solving $f(\Omega_z) = 0$. Our estimate employs the parameters, $M_0 = 1.557 \times 10^5$ A/m, $\alpha = 6.7 \times 10^{-5}$, $H_0 = 2.6 \times 10^5$ A/m, of a spin pumping experiment for yttrium iron garnet (YIG) [62].

Before showing our results, we should explain that both stable and unstable solutions may appear in general. Figure 1(b) is a schematic graph of $f(\Omega_z)$ and the solutions of $f(\Omega_z) = 0$ when $f(\Omega_z)$ has three solutions, $\Omega_{z,i}$ ($i = 1, 2, 3$). Two solutions, $\Omega_{z,1}$ and $\Omega_{z,3}$, are stable because an infinitesimal change in Ω_z induces a restoring torque. On the other hand, $\Omega_{z,2}$ is an unstable solution because no restoring torque works there. The emergence of three solutions highly depends on the microwave amplitude h and the Gilbert damping parameter α , as will be discussed later. Hereafter, we calculate the steady-state rotation frequency as a function of the microwave frequency ω and study how it changes as h varies.

Figures 2(a)–2(d) show the rotation frequency of the steady state as a function of the microwave frequency for $h = 4$ A/m. The red and blue curves indicate the stable and unstable solutions, respectively. For a sufficiently high pressure, only one solution can be realized for arbitrary microwave frequencies (not shown in Fig. 2). As the pressure is lowered, two stable solutions and one unstable solution appear [Fig. 2(a)]. These solutions produced by bifurcation appear only near the

resonant frequency $\omega_0 = -\mu_0\gamma H_0 \simeq 57.52$ GHz, while one stable solution exists away from the resonant frequency. As the pressure is lowered, the lower stable branch approaches the upper one and they become connected to each other at a certain pressure, p_1 [Fig. 2(b)]. Below this critical pressure, the topology of the graph of Ω_z changes [Fig. 2(c)], and a transition from the lower to the upper branch becomes possible when the microwave frequency ω approaches ω_0 . For a sufficiently low pressure, the bifurcation disappears and only one stable solution exists for any microwave frequency [Fig. 2(d)]. In order to see the characteristics of the branches, we show the magnetization of the particle at the critical pressure in Fig. 2(e). The particle has a small (large) magnetization in the upper (lower) branch with a large (small) steady-state rotation frequency. This means that the distribution of the angular momentum between magnetization and rigid-body rotation is different in these two branches.

Figure 2(f) shows the steady-state solutions at $\omega = \omega_0$ in p - Ω_z space. The green area in the figure is the forbidden region in which M_z becomes an imaginary number. The critical pressure is defined as the lowest pressure in the lower branch in Fig. 2(f) and is calculated as [55]

$$p_1 = \frac{4|\gamma|\mu_0^2 M_0 h^2}{r\alpha\omega_0^2} \sqrt{\frac{\pi k_B T}{2m_{\text{air}}}}. \quad (7)$$

In the present estimate, the critical pressure at $h = 4$ A/m is $p_1 \simeq 4.4 \times 10^{-3}$ Pa.

Figures 2(g)–2(j) show the steady-state rotation frequency for $h = 12$ A/m. In this case, there is no bifurcation and only one stable solution at any frequency and any pressure. Note that the graph of Ω_z has a cusp at $\omega = \omega_0$ at a specific pressure $p = p_2$. At this pressure, the magnetization reaches zero at $\omega = \omega_0$ [Fig. 2(k)]. The bifurcation disappears because the unstable solutions are inside the forbidden region, as shown in Fig. 2(l) which plots the steady-state solutions at $\omega = \omega_0$ on the p - Ω_z plane. The pressure $p = p_2$ corresponds to the crossing point of the two solutions, which is always on the boundary of the forbidden region [55]. Finally, we should note that for $g_{\text{SR}} = 1$ the ferromagnetic resonance frequency is not affected by the rotation frequency. This is because the decrease in microwave frequency in the rotating frame [see Eq. (2)] is completely compensated by the decrease in the effective magnetic field due to the spin-rotation coupling (the Barnett effect) through the LLG equation (3).

Thus, whether or not the bifurcation occurs depends on the pressure. The condition for a bifurcation to appear is obtained by solving $p_1 < p_2$ at $\omega = \omega_0$ as $h/H_0 < \alpha/2$ [55]. This indicates the bifurcation disappears at high microwave amplitudes, which is consistent with the results shown in Fig. 2.

Now, let us consider the case when g_{SR} deviates from 1. Figure 3 shows the rotation frequency as a function of the microwave frequency ω for different values of g_{SR} for $p = p_1$ and $h = 4$ A/m. The curves are strongly tilted even for a small deviation in g_{SR} from 1. Furthermore, even when $g_{\text{SR}} = 1$ is small [see Figs. 3(c) and 3(d)], the two stable branches exist in a finite range of ω ; therefore, transitions from the lower branch to the upper branch always occur as ω changes, for example, $\omega \simeq 57.51$ GHz in Fig. 3(c). These changes originate from

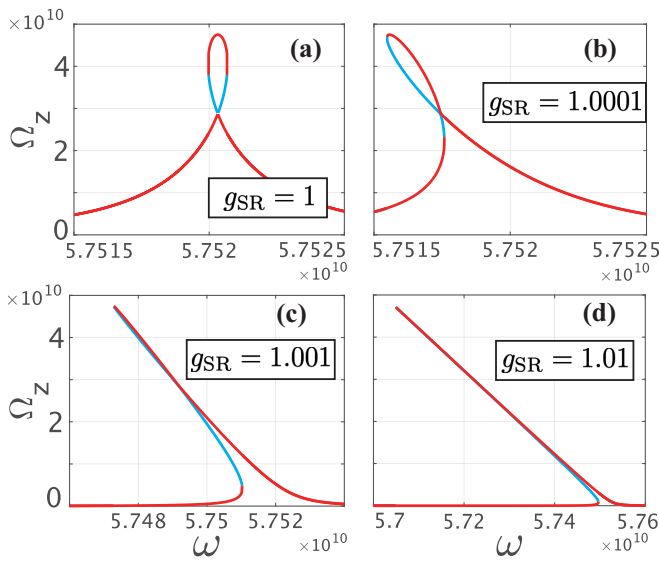


FIG. 3. Steady-state solutions for the rotation frequency Ω_z for various g_{SR} : (a) $g_{SR} = 1$, (b) $g_{SR} = 1.0001$, (c) $g_{SR} = 1.001$, and (d) $g_{SR} = 1.01$. The pressure and microwave amplitude are fixed: $p = p_1$ and $h = 4$ A/m. Red (blue) curves are stable (unstable). The scale of the horizontal axis is different in each figure.

incomplete compensation between the microwave frequency shift and the spin-rotation coupling in the rotating frame. This behavior can be utilized for measuring the effective g factor of the spin-rotation coupling. Note that if $g_{SR} - 1$ is negative, the graph of $\Omega_z(\omega)$ is tilted in the opposite direction.

Conclusion. We examined angular-momentum transfer between the spins and the mechanical angular momentum of a levitated ferromagnetic particle driven by microwave irradiation in a vacuum. This setup is suitable not only for making precise measurements but also for very fast mechanical rotation, due to the absence of a restoring torque, as shown

in recent experiments on levitated optomechanics [35]. We formulated the steady-state rotation frequency using the LLG equation in combination with angular-momentum conservation and estimated it using realistic experimental parameters. We found a bifurcation phenomenon in the solutions for the steady-state rotation frequency when the rotation frequency is very fast and comparable to the microwave frequency. Our setup is a great candidate for satisfying these conditions, which are essential for the strong Barnett effect, in other words, coexistence of the Barnett and the EdH effects. When the g factor for the spin-rotation coupling, g_{SR} , is unity, a transition in rotation frequency is observed near the resonant frequency due to transitions between the two branches. Even a slight deviation in the g -factor g_{SR} from unity separates the two branches more significantly and the transition in rotation frequency appears in a wider region of pressure. This feature of a bifurcation sensitive to the value of g_{SR} can be used for accurate measurement for the effective g factor. Our proposal will provide a powerful way to investigate angular-momentum conversion from magnetism to macroscopic motion in ferromagnets and will promote interdisciplinary research between two developing research fields, spintronics and optomechanics.

Acknowledgments. We thank Y. Ominato, H. Taya, and M. Hongo for helpful comments. We acknowledge JSPS KAKENHI for Grants No. JP20K03831, No. JP21K03414, No. JP21H04565, No. JP21H01800, No. JP23H01839, and No. JP23KJ0702. M.M. is partially supported by the Priority Program of the Chinese Academy of Sciences, Grant No. XDB28000000. D.O. is supported by the President's Ph.D. Scholarships at Imperial College London, by JSPS Overseas Research Fellowship, by the Institution of Engineering and Technology (IET), and by Fundação para a Ciência e a Tecnologia and Instituto de Telecomunicações under Project No. UIDB/50008/2020. T.S. was supported by the Japan Society for the Promotion of Science through the Program for Leading Graduate Schools (MERIT).

- [1] S. J. Barnett, Magnetization by rotation, *Phys. Rev.* **6**, 239 (1915).
- [2] A. Einstein and W. J. de Haas, Experimental proof of the existence of Ampère's molecular currents, *KNAW Proc.* **181**, 696 (1915).
- [3] G. G. Scott, Review of gyromagnetic ratio experiments, *Rev. Mod. Phys.* **34**, 102 (1962).
- [4] K. Harii, Y.-J. Seo, Y. Tsutsumi, H. Chudo, K. Oyanagi, M. Matsuo, Y. Shiomi, T. Ono, S. Maekawa, and E. Saitoh, Spin Seebeck mechanical force, *Nat. Commun.* **10**, 2616 (2019).
- [5] K. Mori, M. G. Dunsmore, J. E. Losby, D. M. Jenson, M. Belov, and M. R. Freeman, Einstein-de Haas effect at radio frequencies in and near magnetic equilibrium, *Phys. Rev. B* **102**, 054415 (2020).
- [6] M. Matsuo, J. Ieda, E. Saitoh, and S. Maekawa, Effects of Mechanical Rotation on Spin Currents, *Phys. Rev. Lett.* **106**, 076601 (2011).
- [7] M. Matsuo, J. Ieda, K. Harii, E. Saitoh, and S. Maekawa, Mechanical generation of spin current by spin-rotation coupling, *Phys. Rev. B* **87**, 180402(R) (2013).
- [8] A. Hirohata, Y. Baba, B. A. Murphy, B. Ng, Y. Yao, K. Nagao, and J.-y. Kim, Magneto-optical detection of spin accumulation under the influence of mechanical rotation, *Sci. Rep.* **8**, 1974 (2018).
- [9] R. Takahashi, M. Matsuo, M. Ono, K. Harii, H. Chudo, S. Okayasu, J. Ieda, S. Takahashi, S. Maekawa, and E. Saitoh, Spin hydrodynamic generation, *Nat. Phys.* **12**, 52 (2016).
- [10] R. Takahashi, H. Chudo, M. Matsuo, K. Harii, Y. Ohnuma, S. Maekawa, and E. Saitoh, Giant spin hydrodynamic generation in laminar flow, *Nat. Commun.* **11**, 3009 (2020).
- [11] H. Tabaei Kazerooni, A. Thieme, J. Schumacher, and C. Cierpka, Electron Spin-Vorticity Coupling in Pipe Flows at Low and High Reynolds Number, *Phys. Rev. Appl.* **14**, 014002 (2020).
- [12] H. Tabaei Kazerooni, G. Zinchenko, J. Schumacher, and C. Cierpka, Electrical voltage by electron spin-vorticity coupling in laminar ducts, *Phys. Rev. Fluids* **6**, 043703 (2021).
- [13] D. Kobayashi, T. Yoshikawa, M. Matsuo, R. Iguchi, S. Maekawa, E. Saitoh, and Y. Nozaki, Spin Current Generation

- Using a Surface Acoustic Wave Generated via Spin-Rotation Coupling, *Phys. Rev. Lett.* **119**, 077202 (2017).
- [14] Y. Kurimune, M. Matsuo, S. Maekawa, and Y. Nozaki, Highly nonlinear frequency-dependent spin-wave resonance excited via spin-vorticity coupling, *Phys. Rev. B* **102**, 174413 (2020).
- [15] S. Tateno, G. Okano, M. Matsuo, and Y. Nozaki, Electrical evaluation of the alternating spin current generated via spin-vorticity coupling, *Phys. Rev. B* **102**, 104406 (2020).
- [16] S. Tateno, Y. Kurimune, M. Matsuo, K. Yamanoi, and Y. Nozaki, Einstein–de Haas phase shifts in surface acoustic waves, *Phys. Rev. B* **104**, L020404 (2021).
- [17] The STAR Collaboration, Global Λ hyperon polarization in nuclear collisions, *Nature (London)* **548**, 62 (2017).
- [18] J. Adam, L. Adamczyk, J. R. Adams, J. K. Adkins, G. Agakishiev, M. M. Aggarwal, Z. Ahammed, N. N. Ajitanand, I. Alekseev, D. M. Anderson *et al.*, Global polarization of Λ hyperons in Au+Au collisions at $\sqrt{s_{NN}} = 200$ GeV, *Phys. Rev. C* **98**, 014910 (2018).
- [19] J. Adam, L. Adamczyk, J. R. Adams, J. K. Adkins, G. Agakishiev, M. M. Aggarwal, Z. Ahammed, I. Alekseev, D. M. Anderson, R. Aoyama *et al.*, Polarization of Λ ($\bar{\Lambda}$) Hyperons along the Beam Direction in Au+Au Collisions at $\sqrt{s_{NN}} = 200$ GeV, *Phys. Rev. Lett.* **123**, 132301 (2019).
- [20] S. Acharya, D. Adamová, A. Adler, J. Adolfsson, M. M. Aggarwal, G. A. Rinella, M. Agnello, N. Agrawal, Z. Ahammed, S. Ahmad *et al.*, Evidence of Spin-Orbital Angular Momentum Interactions in Relativistic Heavy-Ion Collisions, *Phys. Rev. Lett.* **125**, 012301 (2020).
- [21] J. Adam, L. Adamczyk, J. R. Adams, J. K. Adkins, G. Agakishiev, M. M. Aggarwal, Z. Ahammed, I. Alekseev, D. M. Anderson, A. Aparin *et al.*, Global Polarization of Ξ and Ω Hyperons in Au+Au Collisions at $\sqrt{s_{NN}} = 200$ GeV, *Phys. Rev. Lett.* **126**, 162301 (2021).
- [22] T. M. Wallis, J. Moreland, and P. Kabos, Einstein–de Haas effect in a NiFe film deposited on a microcantilever, *Appl. Phys. Lett.* **89**, 122502 (2006).
- [23] G. Zolfagharkhani, A. Gaidarzhly, P. Degiovanni, S. Kettemann, P. Fulde, and P. Mohanty, Nanomechanical detection of itinerant electron spin flip, *Nat. Nanotechnol.* **3**, 720 (2008).
- [24] M. Imai, Y. Ogata, H. Chudo, M. Ono, K. Harii, M. Matsuo, Y. Ohnuma, S. Maekawa, and E. Saitoh, Observation of gyromagnetic reversal, *Appl. Phys. Lett.* **113**, 052402 (2018).
- [25] M. Imai, H. Chudo, M. Ono, K. Harii, M. Matsuo, Y. Ohnuma, S. Maekawa, and E. Saitoh, Angular momentum compensation manipulation to room temperature of the ferrimagnet $\text{Ho}_{3-x}\text{Dy}_x\text{Fe}_5\text{O}_{12}$ detected by the Barnett effect, *Appl. Phys. Lett.* **114**, 162402 (2019).
- [26] C. Dornes, Y. Acremann, M. Savoini, M. Kubli, M. J. Neugebauer, E. Abreu, L. Huber, G. Lantz, C. A. F. Vaz, H. Lemke, E. M. Bothschafter, M. Porer, V. Esposito, L. Rettig, M. Buzzi, A. Alberca, Y. W. Windsor, P. Beaud, U. Staub, D. Zhu *et al.*, The ultrafast Einstein–de Haas effect, *Nature (London)* **565**, 209 (2019).
- [27] W. Izumida, R. Okuyama, K. Sato, T. Kato, and M. Matsuo, Einstein–de Haas Nanorotor, *Phys. Rev. Lett.* **128**, 017701 (2022).
- [28] F. W. Hehl and W.-T. Ni, Inertial effects of a Dirac particle, *Phys. Rev. D* **42**, 2045 (1990).
- [29] J. Fröhlich and U. M. Studer, Gauge invariance and current algebra in nonrelativistic many-body theory, *Rev. Mod. Phys.* **65**, 733 (1993).
- [30] A. Ashkin, Acceleration and Trapping of Particles by Radiation Pressure, *Phys. Rev. Lett.* **24**, 156 (1970).
- [31] A. Ashkin and J. M. Dziedzic, Optical levitation in high vacuum, *Appl. Phys. Lett.* **28**, 333 (1976).
- [32] A. Ashkin, J. M. Dziedzic, J. E. Bjorkholm, and S. Chu, Observation of a single-beam gradient force optical trap for dielectric particles, *Opt. Lett.* **11**, 288 (1986).
- [33] S. Chu, L. Hollberg, J. E. Bjorkholm, A. Cable, and A. Ashkin, Three-Dimensional Viscous Confinement and Cooling of Atoms by Resonance Radiation Pressure, *Phys. Rev. Lett.* **55**, 48 (1985).
- [34] V. Vuletić and S. Chu, Laser Cooling of Atoms, Ions, or Molecules by Coherent Scattering, *Phys. Rev. Lett.* **84**, 3787 (2000).
- [35] C. Gonzalez-Ballesteros, M. Aspelmeyer, L. Novotny, R. Quidant, and O. Romero-Isart, Levitodynamics: Levitation and control of microscopic objects in vacuum, *Science* **374**, eabg3027 (2021).
- [36] T. Li, S. Kheifets, and M. G. Raizen, Millikelvin cooling of an optically trapped microsphere in vacuum, *Nat. Phys.* **7**, 527 (2011).
- [37] J. Gieseler, B. Deutsch, R. Quidant, and L. Novotny, Subkelvin Parametric Feedback Cooling of a Laser-Trapped Nanoparticle, *Phys. Rev. Lett.* **109**, 103603 (2012).
- [38] V. Jain, J. Gieseler, C. Moritz, C. Dellago, R. Quidant, and L. Novotny, Direct Measurement of Photon Recoil from a Levitated Nanoparticle, *Phys. Rev. Lett.* **116**, 243601 (2016).
- [39] D. E. Chang, C. A. Regal, S. B. Papp, D. J. Wilson, J. Ye, O. Painter, H. J. Kimble, and P. Zoller, Cavity opto-mechanics using an optically levitated nanosphere, *Proc. Natl. Acad. Sci. USA* **107**, 1005 (2010).
- [40] J. Millen, P. Z. G. Fonseca, T. Mavrogordatos, T. S. Monteiro, and P. F. Barker, Cavity Cooling a Single Charged Levitated Nanosphere, *Phys. Rev. Lett.* **114**, 123602 (2015).
- [41] F. Tebbenjohanns, M. Frimmer, V. Jain, D. Windey, and L. Novotny, Motional Sideband Asymmetry of a Nanoparticle Optically Levitated in Free Space, *Phys. Rev. Lett.* **124**, 013603 (2020).
- [42] R. Reimann, M. Doderer, E. Hebestreit, R. Diehl, M. Frimmer, D. Windey, F. Tebbenjohanns, and L. Novotny, GHz Rotation of an Optically Trapped Nanoparticle in Vacuum, *Phys. Rev. Lett.* **121**, 033602 (2018).
- [43] J. Ahn, Z. Xu, J. Bang, Y.-H. Deng, T. M. Hoang, Q. Han, R.-M. Ma, and T. Li, Optically Levitated Nanodumbbell Torsion Balance and GHz Nanomechanical Rotor, *Phys. Rev. Lett.* **121**, 033603 (2018).
- [44] Y. Arita, M. Mazilu, and K. Dholakia, Laser-induced rotation and cooling of a trapped microgyroscope in vacuum, *Nat. Commun.* **4**, 2374 (2013).
- [45] J. Čimurs and A. Čēbers, Three-dimensional dynamics of a particle with a finite energy of magnetic anisotropy in a rotating magnetic field, *Phys. Rev. E* **88**, 062315 (2013).
- [46] J. Čimurs and A. Čēbers, Dynamics of anisotropic superparamagnetic particles in a precessing magnetic field, *Phys. Rev. E* **87**, 062318 (2013).

- [47] K. D. Usadel, Dynamics of magnetic nanoparticles in a viscous fluid driven by rotating magnetic fields, *Phys. Rev. B* **95**, 104430 (2017).
- [48] K. D. Usadel and C. Usadel, Dynamics of magnetic single domain particles embedded in a viscous liquid, *J. Appl. Phys.* **118**, 234303 (2015).
- [49] N. A. Usov and B. Y. Liubimov, Magnetic nanoparticle motion in external magnetic field, *J. Magn. Magn. Mater.* **385**, 339 (2015).
- [50] N. A. Usov and B. Y. Liubimov, Dynamics of magnetic nanoparticle in a viscous liquid: Application to magnetic nanoparticle hyperthermia, *J. Appl. Phys.* **112**, 023901 (2012).
- [51] H. Keshtgar, S. Streib, A. Kamra, Y. M. Blanter, and G. E. W. Bauer, Magnetomechanical coupling and ferromagnetic resonance in magnetic nanoparticles, *Phys. Rev. B* **95**, 134447 (2017).
- [52] T. V. Lyutyy, O. M. Hryshko, and M. Y. Yakovenko, Uniform and nonuniform precession of a nanoparticle with finite anisotropy in a liquid: Opportunities and limitations for magnetic fluid hyperthermia, *J. Magn. Magn. Mater.* **473**, 198 (2019).
- [53] T. V. Lyutyy, S. I. Denisov, and P. Hänggi, Dissipation-induced rotation of suspended ferromagnetic nanoparticles, *Phys. Rev. B* **100**, 134403 (2019).
- [54] P. Huillery, T. Delord, L. Nicolas, M. Van Den Bossche, M. Perdriat, and G. Hétet, Spin mechanics with levitating ferromagnetic particles, *Phys. Rev. B* **101**, 134415 (2020).
- [55] See Supplemental Material at <http://link.aps.org/supplemental/10.1103/PhysRevB.107.L180406> for experimental implementation, detailed calculations of the air resistance, the angular-momentum conservation law, the critical pressure, effect of the Gilbert damping, g factor for the spin-rotation coupling, and stability analysis of the rotation, which contains Refs. [42–44,54,58–60,63,64].
- [56] C. Kittel, On the theory of ferromagnetic resonance absorption, *Phys. Rev.* **73**, 155 (1948).
- [57] M. Matsuo, J. Ieda, and S. Maekawa, Renormalization of spin-rotation coupling, *Phys. Rev. B* **87**, 115301 (2013).
- [58] P. S. Epstein, On the resistance experienced by spheres in their motion through gases, *Phys. Rev.* **23**, 710 (1924).
- [59] A. Roth, *Vacuum Technology* (North-Holland, Amsterdam, 1990).
- [60] J. Corson, G. W. Mulholland, and M. R. Zachariah, Calculating the rotational friction coefficient of fractal aerosol particles in the transition regime using extended Kirkwood-Riseman theory, *Phys. Rev. E* **96**, 013110 (2017).
- [61] In our estimate, a fluctuation of rotation velocity, which is dominantly induced by thermal fluctuation of air resistance torque, becomes much smaller than its average. Therefore, the noise of rotation frequency does not affect its precious measurement.
- [62] Y. Kajiwara, K. Harii, S. Takahashi, J. Ohe, K. Uchida, M. Mizuguchi, H. Umezawa, H. Kawai, K. Ando, K. Takanashi, S. Maekawa, and E. Saitoh, Transmission of electrical signals by spin-wave interconversion in a magnetic insulator, *Nature (London)* **464**, 262 (2010).
- [63] F. Monteiro, S. Ghosh, E. C. van Assendelft, and D. C. Moore, Optical rotation of levitated spheres in high vacuum, *Phys. Rev. A* **97**, 051802(R) (2018).
- [64] R. M. White, *Quantum Theory of Magnetism* (Springer, Berlin, Heidelberg, 2007).